Hardware-in-the-Loop Evaluation for Potential High Limit Estimation-Based PV Plant Active Control

Preprint

Mengmeng Cai,[1] Simon Julien,[2] Jing Wang,[1] Subhankar Ganguly,[1] Weihang Yan,[1] Zachary Jacobs,[2] Tristan Liu,[2] and Vahan Gevorgian[1]

1 National Renewable Energy Laboratory
2 Latimer Controls

To be presented at the 2024 IEEE Power & Energy Society General Meeting
Seattle, Washington
July 21-25, 2024

NREL is a national laboratory of the U.S. Department of Energy
Office of Energy Efficiency & Renewable Energy
Operated by the Alliance for Sustainable Energy, LLC

This report is available at no cost from the National Renewable Energy Laboratory (NREL) at www.nrel.gov/publications.

Contract No. DE-AC36-08GO28308

Conference Paper
NREL/CP-5D00-87998
March 2024

Hardware-in-the-Loop Evaluation for Potential High Limit Estimation-Based PV Plant Active Control

Preprint

Mengmeng Cai,[1] Simon Julien,[2] Jing Wang,[1]
Subhankar Ganguly,[1] Weihang Yan,[1] Zachary Jacobs,[2]
Tristan Liu,[2] and Vahan Gevorgian[1]

1 National Renewable Energy Laboratory
2 Latimer Controls

Suggested Citation
Cai, Mengmeng, Simon Julien, Jing Wang, Subhankar Ganguly, Weihang Yan, Zachary Jacobs, Tristan Liu, and Vahan Gevorgian. 2024. *Hardware-in-the-Loop Evaluation for Potential High Limit Estimation-Based PV Plant Active Control: Preprint*. Golden, CO: National Renewable Energy Laboratory. NREL/CP-5D00-87998. https://www.nrel.gov/docs/fy24osti/87998.pdf.

NREL is a national laboratory of the U.S. Department of Energy
Office of Energy Efficiency & Renewable Energy
Operated by the Alliance for Sustainable Energy, LLC

This report is available at no cost from the National Renewable Energy Laboratory (NREL) at www.nrel.gov/publications.

Contract No. DE-AC36-08GO28308

Conference Paper
NREL/CP-5D00-87998
March 2024

National Renewable Energy Laboratory
15013 Denver West Parkway
Golden, CO 80401
303-275-3000 • www.nrel.gov

NOTICE

This work was authored by the National Renewable Energy Laboratory, operated by Alliance for Sustainable Energy, LLC, for the U.S. Department of Energy (DOE) under Contract No. DE-AC36-08GO28308. Funding provided by the U.S. Department of Energy Office of Energy Efficiency and Renewable Energy Solar Energy Technologies Office. The views expressed herein do not necessarily represent the views of the DOE or the U.S. Government. The U.S. Government retains and the publisher, by accepting the article for publication, acknowledges that the U.S. Government retains a nonexclusive, paid-up, irrevocable, worldwide license to publish or reproduce the published form of this work, or allow others to do so, for U.S. Government purposes.

Cover Photos by Dennis Schroeder: (clockwise, left to right) NREL 51934, NREL 45897, NREL 42160, NREL 45891, NREL 48097, NREL 46526.

Hardware-in-the-Loop Evaluation for Potential High Limit Estimation-Based PV Plant Active Control

Mengmeng Cai, Simon Julien, Jing Wang, Subhankar Ganguly, Weihang Yan, Zachary Jacobs, Tristan Liu, and Vahan Gevorgian

***Abstract*—This paper validates the efficacy of an artificial intelligence (AI)-based photovoltaic (PV) plant control and optimization approach in enabling PV plants as accountable grid reliability service providers. The validation is performed in a realistic laboratory controller-hardware-in-the-loop environment, leveraging accurate PV plant modeling and standard industrial communication protocols. Through simulations that account for diverse weather conditions and active control scenarios, the results highlight the superior performance of the AI-based solution in comparison to a state-of-the-art reference-control grouping-based approach. Such a finding contributes to mitigating the risk of overcurtailment and uninstructed deviations of active PV plant controls, and offers practical guidance for its field deployment. Furthermore, it establishes a standardized testing framework for comparing various PV active control strategies.**

***Index Terms*—PV active control, Hardware-in-the-loop, Potential high limit**

I. Introduction

As utilities strive to meet the 2050 net-zero greenhouse gas emissions target, their solar capacities have substantially increased in recent years and will continue to expand in the coming decades [1]. This surge in renewable energy adoption requires additional system flexibility to address the increasing variability and uncertainty. Traditionally, system flexibility has been provided by fossil-fueled generators; however, with the evolving energy landscape, there is increasing interest in alternative flexible resources, such as actively controlled photovoltaic (PV) plants. Under active control, PV plants can operate at curtailed operation levels and rapidly respond to meet grid service demands at zero marginal cost, offering advantages in enhancing the system efficiency and reducing the strain on conventional generators [2]; however, unlike traditional operating reserve providers, such as fossil-fueled generators, whose operating characteristics (e.g., available operation headroom) are well-defined, PV plants are inherently variable and uncertain. To ensure feasible and efficient coordination between PV plants and the system operator during an active control event, it is essential to accurately estimate the maximum available power output, i.e., potential high limit (PHL), of the plants even when they are being curtailed.

To address this need, the current state-of-the-art method applies a reference-control grouping strategy that reserves part of the inverters (reference group) to operate at their PHLs and dispatches only the remaining inverters (control group) at curtailed levels to fulfill the flexibility need [3]. Despite being successfully demonstrated in the field [4][5], there exist two gaps in the state of the art to fully unlock the flexibility of PV plants: a. There is a trade-off between the PHL estimation accuracy and the flexibility range. b. There lacks granularity in the PHL estimation to capture the variation across inverters.

To tackle these challenges, Latimer Controls proposed an integrated solution combining an artificial intelligence (AI)-based, inverter-level PHL estimation model and a hierarchical inverter control model [6]; however, its performance has been tested only in a software environment, and it has not been comprehensively compared to the state of the art under various operating conditions. To mitigate risks and provide practical guidance for its future field implementation, the National Renewable Energy Laboratory, in collaboration with Latimer Controls, proposed and developed a controller-hardware-in-the-loop (CHIL) framework for PHL estimation-based PV plant active control with following contributions being made:

1) We developed a 135-MW PV plant model with active control interfaces incorporating detailed modeling of individual PV arrays and inverters. It provides the flexibility to account for different levels of solar irradiance variations.
2) We established a CHIL platform tailored for testing and demonstrating PHL estimation-based PV plant active control. It can be used by both plant and system operators to understand the value of flexible PV plants and standardizes the comparison among different technologies.

II. Hardware-in-the-loop setup

A. Overall framework

Fig. 1 illustrates the framework of the proposed CHIL test bed and compares the implementations between the AI-based and baseline (i.e., reference control grouping-based method) solutions. It is built using RTDS and Opal-RT. While RTDS handles the electromagnetic transients (EMT) PV plant modeling at 50 micro-second intervals and acts as the system operator, Opal-RT functions as the prototype plant controller.

B. PV plant under test

To account for the varying cloud conditions and diverse inverter dispatches, we have developed a 135-MW PV plant

M. Cai, J. Wang, S. Ganguly, W. Yan, and V. Gevorgian are with the National Renewable Energy Laboratory, Golden, CO 15013 USA e-mail: mengmeng.cai@nrel.gov.

S. Julien, Z. Jacobs, and T. Liu are with Latimer Controls, Boulder, CO, 80301 USA.

This work was authored in part by the National Renewable Energy Laboratory, operated by Alliance for Sustainable Energy, LLC, for the U.S. Department of Energy (DOE) under Contract No. DE-AC36-08GO28308. Funding provided by U.S. Department of Energy Office of Energy Efficiency and Renewable Energy Solar Energy Technologies Office. The views expressed in the article do not necessarily represent the views of the DOE or the U.S. Government.

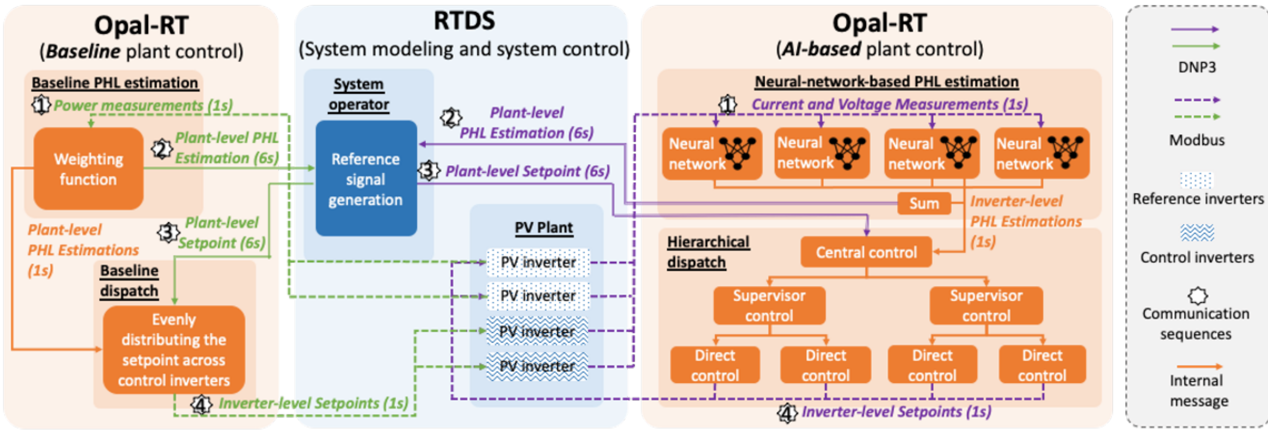

Fig. 1. Illustration of the CHIL framework (four inverters are plotted for illustrative purposes).

with detailed modeling of 27 individual PV modules using RTDS. Each module is paired with a 5-MW/0.48-kV current-regulated voltage source inverter, which is then aggregated to connect with a 345-kV point of common coupling through two step-up transformers, as shown in the upper part of Fig. 2. The details of the inverter control are illustrated in the lower part of Fig. 2. We applied generic DC voltage control, current reference generation and current control functions [7] to form the outer voltage and inner current control loops. A switching function has been added to enable the transition between operating in maximum power point tracking (MPPT) and being actively controlled.

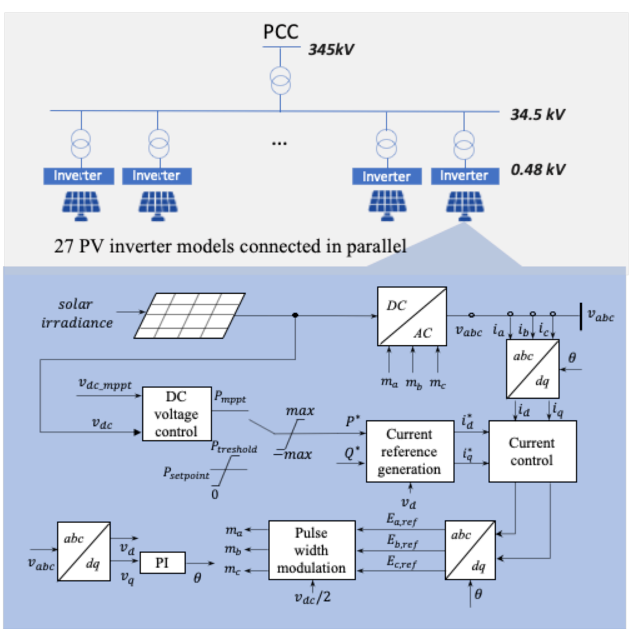

Fig. 2. PV plant modeling. Notations: v_{abc}-three phase voltage measurements; i_{abc}-three phase current measurements; v_{dq}-dq reference frame voltage measurements; i_{dq}-dq reference frame current measurements; V_{dc_mppt}-DC link MPPT voltage reference; v_{dc}-DC link voltage measurement; P_{mppt}-active power reference under MPPT, $P_{setpoint}$- active dispatch set point; $P_{treshold}$-upper bound of the active dispatch set point; P^*, Q^*- active and reactive power references; i_d^*, i_q^*-dq reference frame current references; $E_{a,ref}$, $E_{b,ref}$, $E_{c,ref}$-reference voltages of the inverter legs; m_a, m_b, m_c-modulation signals; θ-voltage angle.

C. Controller under test

The AI-based and baseline plant controllers are hosted in Opal-RT, and both contain a PHL estimation and dispatch functions. Whereas the AI-based solution estimates inverter-level PHLs based on historical DC-side current and voltage measurements from the previous 10 steps for all inverters through neural networks, the baseline solution estimates plant-level PHL based on current AC-side power measurements from all reference inverters through a simple scaling function, as illustrated in Fig. 3. With regard to the dispatch function, whereas the AI-based solution disaggregates the plant-level set point proportionally to the inverter-level PHL estimations, the baseline solution distributes the remaining dispatch set points (plant-level dispatch set point subtracts the sum of the current outputs of reference inverters) among control inverters proportionally to their rated powers, as depicted in Fig. 4. More details about AI-based and baseline solutions can be found in [6], [5].

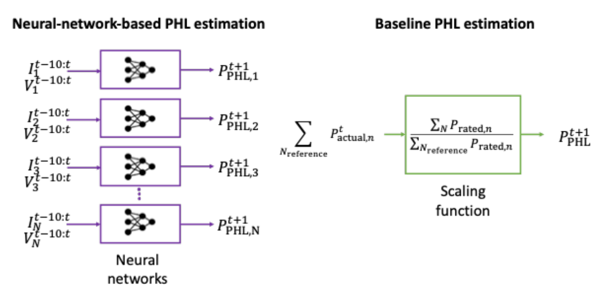

Fig. 3. Comparison of the two PHL estimation approaches. Notations: n-inverter index; t-time index; $P_{\mathrm{PHL},n}^{t+1}$-inverter-level PHL estimation; $I_n^{t-10:t}$ and $V_n^{t-10:t}$-DC-side current and voltage measurements from previous 10 steps; P_{PHL}^{t+1}-plant-level PHL estimation;$P_{\mathrm{actual,n}}^{t}$-AC-side power measurement;$P_{\mathrm{rated,n}}$-rated power; N_{referece}-the set of all reference inverters.

D. Communication setup

Communications between the system operator and the plant controller, as well as between the PV inverters and the plant controller, use Distributed Network Protocol 3 (DNP3) and Modbus, as indicated by the dashed and double lines in Fig.

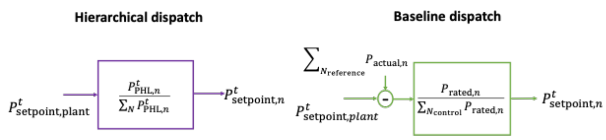

Fig. 4. Comparison of the two dispatch approaches. Notations: $P^t_{\text{setpoint,plant}}$-plant-level dispatch set point; $P^t_{\text{setpoint},n}$-inverter-level dispatch set point of inverter n; N-the set of all inverters; N_{control}-the set of all control inverters.

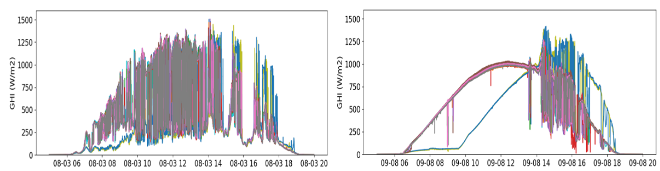

Fig. 5. Solar irradiance profiles for a partially shaded day (left) and a sunny day (right)

1. The PV inverters communicate their measurements and dispatch set points with the plant controller at the second resolution. Every 6 seconds, the plant controller sends an updated plant-level PHL estimation to the system operator in exchange for a plant-level dispatch set point.

III. Case Study

A. Solar irradiance inputs

This study uses the Oahu Solar Measurement Grid data set [8] for the solar irradiance inputs. It offers 1-second resolution measurements of global horizontal irradiance (GHI) from 17 stations in the southwestern region of Oahu. These measurements span 1 year, covering the time from 5 AM to 8 PM daily. Specifically, we chose a partially shaded day and a sunny day from the data set, representing distinct levels of solar irradiance variation. Fig. 5 visualizes the solar irradiance profiles of the two days. Within each day, we selected three 15-min time windows—covering the morning ramp, noon peak, and evening drop—for the simulation.

B. Testing scenarios

To provide a comprehensive evaluation of the performance of the actively controlled PV plant in satisfying different flexibility needs, we implemented four testing scenarios:

(a) Constant generation: Test the capability of maintaining the generation at a fixed value (P_{constant}).
(b) Absolute headroom: Test the capability of maintaining an absolute headroom ($P^{abs}_{\text{headroom}}$).
(c) Percentage headroom: Test the capability of maintaining a percentage headroom ($P^{\%}_{\text{headroom}}$).
(d) Hot-restarting: Stress test the capability of fast ramping down (from t_1 to t_2) and up (from t_2 to t_3) between zero generation and full capacity.

Equations (1)–(4) describe how the $P^t_{\text{setpoint, plant}}$ is determined based on the plant-level PHL estimation, P^t_{PHL}, under each testing scenario:

$$P^t_{\text{setpoint, plant}} = min(P_{\text{constant}}, P^t_{\text{PHL}}) \tag{1}$$

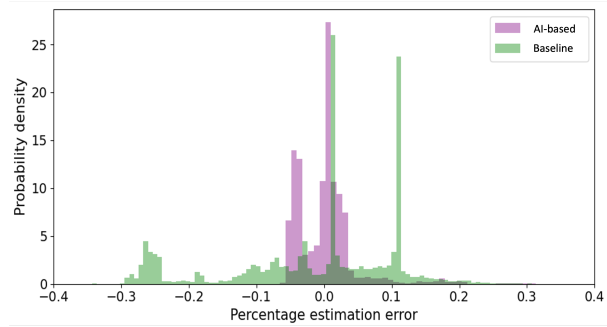

Fig. 6. Distributions of PHL estimation percentage errors

$$P^t_{\text{setpoint, plant}} = P^t_{\text{PHL}} - P^{abs}_{\text{headroom}} \tag{2}$$

$$P^t_{\text{setpoint, plant}} = P^t_{\text{PHL}}(1 - P^{\%}_{\text{headroom}}) \tag{3}$$

$$P^{t_1}_{\text{setpoint, plant}} = P^{t_1}_{\text{PHL}}; P^{t_2}_{\text{setpoint, plant}} = 0; P^{t_3}_{\text{setpoint, plant}} = P^{t_3}_{\text{PHL}} \tag{4}$$

C. Performance metrics

We compared the performance of the AI-based and baseline solutions from the perspectives of PHL estimation accuracy, dispatch precision, overcurtailment, and headroom maintenance by leveraging the following metrics:

$$PEE^t = |P^t_{\text{PHL}} - P^t_{\text{PHL,actual}}|/P^t_{\text{PHL,actual}} \tag{5}$$

$$DE^t = |P^t_{\text{setpoint, plant}} - P^t_{\text{actual}}| \tag{6}$$

$$\begin{aligned} OC^t = max(0, &P^t_{\text{PHL,actual}} - P^t_{\text{actual}}) \\ &- max(0, P^t_{\text{PHL,actual}} - P^t_{\text{setpoint, plant}}) \end{aligned} \tag{7}$$

For testing scenario (b):

$$HD^t = min(0, P^t_{\text{actual}} - (P^t_{\text{PHL,actual}} - P^{abs}_{\text{headroom}})) \tag{8}$$

For testing scenario (c):

$$HD^t = min(0, P^t_{\text{actual}} - P^t_{\text{PHL,actual}} \times (1 - P^{\%}_{\text{headroom}})) \tag{9}$$

where $P^t_{\text{PHL,actual}}$ and P^t_{actual} represent the actual potential high limit and the actual generation at time t. PEE, DE, OC and HD are short for percentage estimation error, dispatch error, overcurtailment, and headroom deviation.

D. Performance evaluation

Fig.6 compares the distributions of the PHL percentage estimation errors, PEE^t, obtained using the neural-network-based and baseline PHL estimation approaches. Compared with the reference control grouping-based method, the neural-network-based method reduces the mean and standard deviation of PEE^t by 70% (from 9.7% to 2.9%) and 63% (from 12.5% to 4.6%).

Table I and Table II compare the averaged DE^t, OC^t, and HD^t obtained using two approaches in two simulation days. Of the 24 runs, 75%, 79%, and 50% of the time, the AI-based solution outperforms the baseline solution in terms of maintaining the dispatch precision, avoiding overcurtailment, and satisfying the headroom requirement. (Cases where the

TABLE I
PERFORMANCE COMPARISON FOR THE SUNNY DAY

		Constant generation		Absolute headroom		Percentage headroom		Hot restarting	
		AI-based	Baseline	AI-based	Baseline	AI-based	Baseline	AI-based	Baseline
Dispatch error (DE^t)	Morning ramp	0.29	4.29	0.19	3.43	0.24	4.39	0.35	6.14
	Noon peak	0.01	0.03	0.52	0.36	0.21	0.45	1.29	3.48
	Evening drop	0.21	0.39	0.13	0.12	0.17	0.19	0.73	0.56
Overcurtailment (OC^t)	Morning ramp	0.29	3.38	0.19	3.43	0.24	4.39	0.35	6.14
	Noon peak	0.00	0.00	0.52	0.36	0.21	0.45	1.29	3.48
	Evening drop	0.19	0.38	0.13	0.12	0.17	0.19	0.73	0.56
Headroom deficiency (HD^t)	Morning ramp	-	-	0.00	1.99	0.00	0.48	-	-
	Noon peak	-	-	1.71	1.91	0.85	1.97	-	-
	Evening drop	-	-	0.11	0.00	0.03	0.00	-	-

TABLE II
PERFORMANCE COMPARISON FOR THE PARTIALLY SHADED DAY

		Constant generation		Absolute headroom		Percentage headroom		Hot restarting	
		AI-based	Baseline	AI-based	Baseline	AI-based	Baseline	AI-based	Baseline
Dispatch error (DE^t)	Morning ramp	0.25	5.41	0.32	1.79	0.20	3.56	0.32	5.92
	Noon peak	1.63	4.55	0.84	2.05	1.32	3.61	2.94	7.24
	Evening drop	0.26	0.15	0.12	0.06	0.22	0.07	0.30	0.33
Overcurtailment (OC^t)	Morning ramp	0.20	2.16	0.32	1.79	0.20	3.56	0.32	5.92
	Noon peak	1.24	3.76	0.84	2.05	1.32	3.61	2.94	7.24
	Evening drop	0.09	0.14	0.12	0.06	0.22	0.07	0.30	0.33
Headroom deficiency (HD^t)	Morning ramp	-	-	0.14	2.12	0.00	0.45	-	-
	Noon peak	-	-	1.70	1.64	0.88	0.72	-	-
	Evening drop	-	-	1.62	0.01	0.36	0.00	-	-

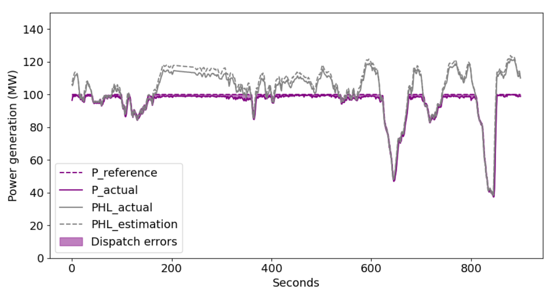

(a) AI-based

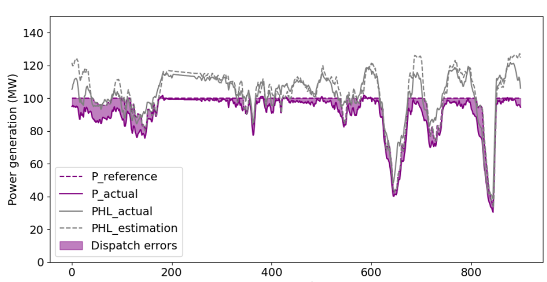

(b) Baseline

Fig. 7. Simulation results for the constant generation testing scenario.

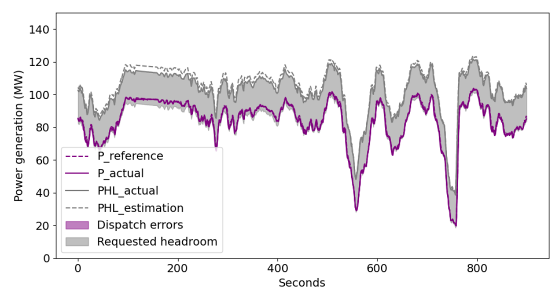

(a) AI-based

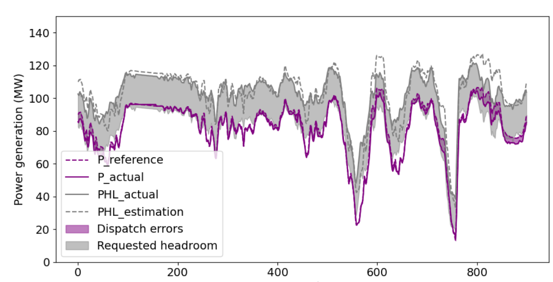

(b) Baseline

Fig. 8. Simulation results for the absolute headroom testing scenario.

AI-based solution underperforms the baseline solution are indicated in blue.)

Figs. 7, 8, 9, 10 further visualize the comparison for the noon peak time window in the partially shaded day under four testing scenarios. It compares the actual PHL, estimated PHL, reference generation, and actual generation time series, with the dispatch error and requested headroom highlighted by the purple and gray areas. A comparison of the subfigures

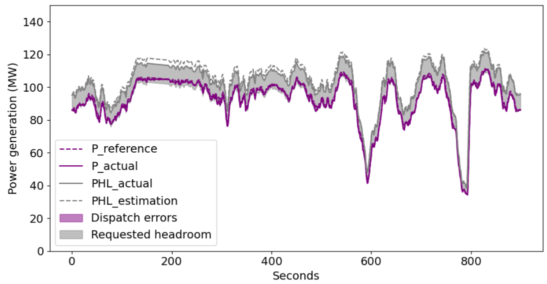

(a) AI-based

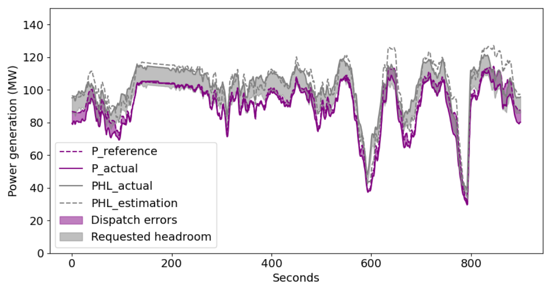

(b) Baseline

Fig. 9. Simulation results for the percentage headroom testing scenario.

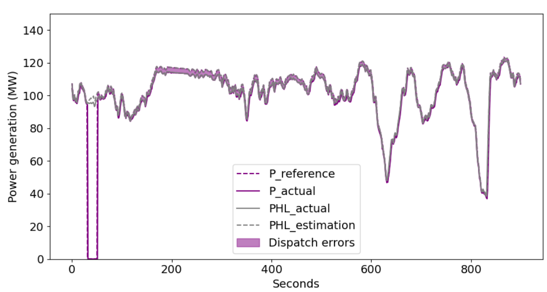

(a) AI-based

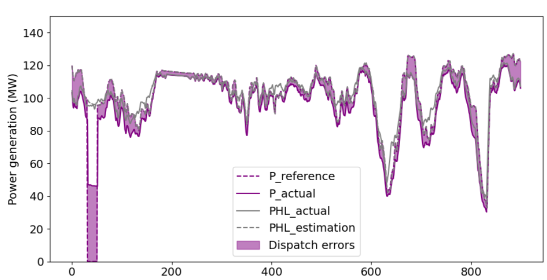

(b) Baseline

Fig. 10. Simulation results for the hot-restarting testing scenario.

in Figs. 7, 8, 9, 10 shows that the shapes of the gray dashed and solid lines are more aligned and the gaps between the two are smaller in Fig. 7a,8a,9a,10a than in Fig. 7b,8b,9b,10b, indicating better PHL estimation performance of the AI-based solution. Moreover, although the reference generations (purple dashed lines) are lower than the actual PHLs (gray solid lines) most of the time in all figures, the purple areas are larger in Figs. 7b,8b,9b,10b than Figs. 7a,8a,9a,10a, indicating that the knowledge of inverter-level PHLs is critical to ensure the dispatch precision. Note that there is a huge dispatch error during the shutoff window (between 30 s and 50 s) of the hot-restarting testing scenario in Fig. 10b, which indicates the restricted flexibility of the reference control grouping-based method given that half of the inverters are reserved to operate at MPPT. This issue can be overcome by the AI-based solution, as shown in Fig. 10a by the actual power rapidly changing between zero and full capacity.

IV. Conclusions and Future Work

This paper introduced a CHIL framework to validate an AI-based PV plant control solution. The simulation results exhibit the AI-based solution's potential in bolstering PV plant reliability as a flexibility provider compared to existing methods. The proposed CHIL framework can be extended to standardize the validation and comparison for various PHL estimation-based PV plant active control strategies. Note this work represents only a preliminary comparison of the two approaches, given the limited time windows that are simulated. In future work, we will: 1. Conduct long-duration simulations to provide more generalized observations. 2. Refine the AI-based PHL estimation using transfer learning. 3. Conduct closed-loop tests. 4. Extend the application to reactive power PHL estimation and voltage support.

References

[1] Implementation and action toward net zero. https://www.southerncompany.com/content/dam/southern-company/pdf/public/Net-zero-report.pdf. Accessed: 2023-10-17.

[2] Mahesh Morjaria, Dmitriy Anichkov, Vladimir Chadliev, and Sachin Soni. A grid-friendly plant: The role of utility-scale photovoltaic plants in grid stability and reliability. *IEEE Power and Energy Magazine*, 12(3):87–95, 2014.

[3] Vahan Gevorgian. Highly accurate method for real-time active power reserve estimation for utility-scale photovoltaic power plants. Technical report, National Renewable Energy Lab.(NREL), Golden, CO (United States), 2019.

[4] Vahan Gevorgian and Barbara O'Neill. Advanced grid-friendly controls demonstration project for utility-scale pv power plants. Technical report, National Renewable Energy Lab.(NREL), Golden, CO (United States), 2016.

[5] Clyde Loutan, Peter Klauer, Sirajul Chowdhury, Stephen Hall, Mahesh Morjaria, Vladimir Chadliev, Nick Milam, Christopher Milan, and Vahan Gevorgian. Demonstration of essential reliability services by a 300-mw solar photovoltaic power plant.

[6] Simon A. Julien, Amirhossein Sajadi, and Bri-Mathias Hodge. Hierarchical control of utility-scale solar pv plants for mitigation of generation variability and ancillary service provision. *IEEE Transactions on Sustainable Energy*, 13(3):1383–1395, 2022.

[7] Amirnaser Yazdani and Reza Iravani. *Voltage-sourced converters in power systems: modeling, control, and applications*. John Wiley & Sons, 2010.

[8] Manajit Sengupta and Afshin Andreas. Oahu solar measurement grid (1-year archive): 1-second solar irradiance; oahu, hawaii (data). *NREL Data Catalog*, 2014. Last updated: September 16, 2022.